EFFECT OF ROTOR ECCENTRICITY FAULTS ON NOISE GENERATION IN PERMANENT MAGNET SYNCHRONOUS MOTORS

A. Rezig [†] **and M. R Mekideche**

LAMEL Laboratory
Jijel University
BP 98 Ouled Aissa, 18000 Jijel, Algeria

A. Djerdir

SET Laboratory
University of Technology Belfort-Montbeliard
13 Rue Thierry Mieg, 90000 Belfort, France

Abstract—Vibrations and noise in electrical machines are directly related to the characteristics of the radial forces on one hand, and mechanical behavior on the other. The characteristics of these forces depend on the air gap flux density, and they are influenced by other factors such as stator slots and poles, saturation level, winding type and certain faults. The aim of this work is to investigate the effect of eccentricity faults on electromagnetic noise generated by the external surface of PM synchronous machine (PMSM). For this purpose an analytical electromagnetic vibroacoustic model is developed. The results confirm the effect of eccentricity fault in generating some low modes radial forces. An experimental device is installed to validate the results of the analytical model.

1. INTRODUCTION

Permanent magnet synchronous motors (PMSM) have many advantages over brushed DC motors and induction Motors. These motors are used in many applications such as traction with variable speeds

in transportation. However, the operation of theses motors is accompanied by unavoidable production of noise especially in the presence of faults which are caused by tolerance in manufacture and assembly. Faults such as eccentricities causes a uniform air gap, corresponding non uniform air gap magnetic field and unbalanced magnetic force on stator producing noise and vibrations. Several works was published in last years about noise and vibration of PM motors [1, 3, 4], however, less research has been observed in vibroacoustic behavior of these motors in relation with eccentricities faults [2]. Authors in [2] demonstrate that eccentricities can contribute to the generation of force with low mode number; however the model is based on a simple calculation of mechanical and acoustic quantity and the authors did not indicate how to validate experimentally the model of eccentricity. The aim of this research is to consider the effect of eccentricities faults on the noise radiated from the permanent magnet machine, this faults are characterized by a signature in the motor sound power level spectrum. For this purpose an analytical electromagnetic vibroacoustic approach to calculate the sound power level radiated from the PM motor is presented. The effect of eccentricity is introduced through the expression of the relative permeance. The analytic approach adopted in this work consider that the magnetic flux density in the air gap of PMSM machine is the product of magnetic flux density generated by rotor magnet (or stator winding) and the relative permeance which take into account the effect of slots [6, 7], the model calculates also the natural frequency of the stator and frame, stator yoke and frame displacements corresponding to the frequency of forces, and noise in the surrounding medium. All parts of the analytical model are validated by FEM simulations, this allows us to adjust and improve the model. The paper propose also a technique to validate the model of eccentricity experimentally, for this purpose the rotor is unbalanced by mounting a slotted disk on the shaft of the PMSM.

2. AIR GAP MAGNETIC FLUX DENSITY AND RADIAL FORCES WAVES

Analytically the magnetic flux density in the air gap of PMSM machine is the product of magnetic flux density generated by rotor magnet (or stator windings) and the relative permeance functions which take into account the effect of slots and eccentricity faults.

$$B(\theta, t) = [B_{magnet}(\theta, t) + B_w(\theta, t)]\bar{\lambda}(\theta) = B_{open\_circuit}(\theta, t) + B_{ar}(\theta, t) \quad (1)$$

where $B_{magnet}(\theta, t)$ and $B_w(\theta, t)$ are the open circuit field produced by magnet and stator windings respectively when the stator slotting

is neglected. Both of $B_{magnet}(\theta, t)$ and $B_w(\theta, t)$ are calculated analytically from 2-d models in polar coordinates. $\bar{\lambda}(\theta)$ is relative permeance which take into account the effect of slots [2]. In practice and for most PMSM motor harmonics in open circuit magnetic field have dominant role in the noise of electromagnetic origin [1, 2]. Open circuit field calculated for a 1.5 kW, 4 poles, 36 slots brushless motors is performed by analytical model and validated by FEM simulations using FLUX software. The results are presented in Figures 1 and 2. In a typical machine with unsaturated conditions; the flux lines are perpendicular to the iron surface. Therefore the tangential component of flux density can be neglected. The radial pressure between stator and rotor surfaces can thus be written as [1, 2, 4]:

$$P_r = \frac{B^2(\theta, t)}{2\mu_0} \tag{2}$$

$$P_r = \frac{\left[B_{magnet}^2(\theta, t) + 2B_w(\theta, t)B_{magnet}(\theta, t) + B_w^2(\theta, t)\right]\bar{\lambda}(\theta)^2}{2\mu_0} \tag{3}$$

In Equation (3), there are three group of infinite number of radial forces waves, each force wave can be expressed in the following general
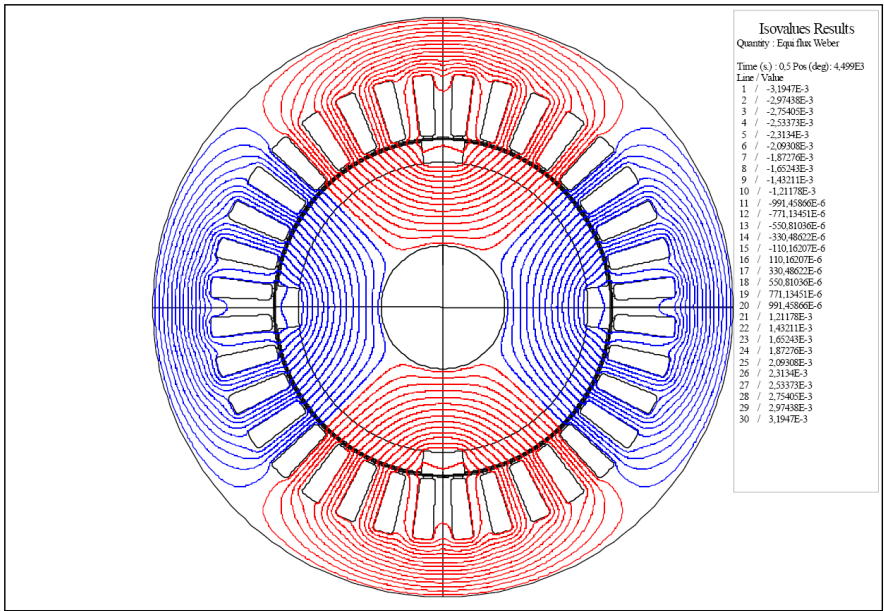

Figure 1. Distribution of magnetic flux density in PM machine obtained by FLUX simulation software.
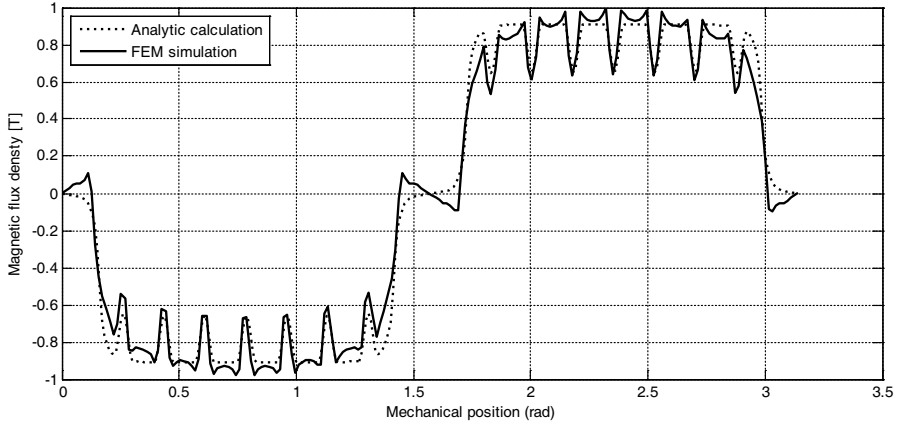
Figure 2. Magnetic flux density in the air-gap of the motor.

form

$$P_r(\theta, t) = P_{mr} \cos(r\theta - w_r t - \theta_r) \qquad (4)$$

where P_{mr} is amplitude of the magnetic pressure, w_r is the angular frequency and $r = 0, 1, 2, 3, 4, \ldots$ are corresponding modes of radial magnetic force.

By only considering the pure circumferential vibration modes of the stator core, the deflection of stator core is an inverse function of the fourth power of the force order r, so the most important from airborne noise point of view are low circumferential mode number. Faults such as eccentricity and demagnetization of permanent magnet in PMSM motors contribute to generation of low mode vibration. The magnetic field calculated above in the case of faults contains additional harmonics giving rise to others harmonics forces waves.

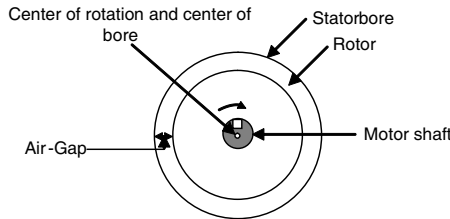## 3. ROTOR ECCENTRICITY FAULTS, DEFINITIONS, CAUSES AND MODELING

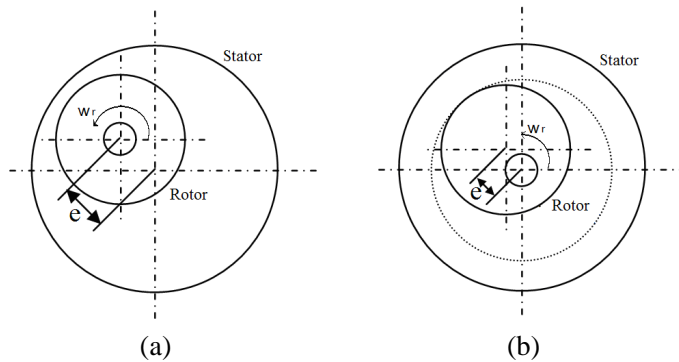**Figure 3.** Ideal motor (no-eccentric air-gap).

Figure 4. Rotor eccentricity (a) static, (b) dynamic.

In ideal machine, the rotor is center-aligned with the stator bore, and the rotor's center of rotation is the same as the geometric center of the stator bore as shown in Figure 3. A rotor eccentricity is a condition of unequal air gap that exists between the stator and the rotor [5]. Air-gap eccentricity can occur in the form of static or dynamic eccentricity. In the case of a static eccentricity, the position of minimum radial air-gap length is fixed in space.

Typical cause of static eccentricity includes stator core ovality or incorrect positioning of the rotor or the stator at the commissioning stage. A dynamic eccentricity occurs when the center of the rotor is not at the center of rotation and minimum air gap revolves with the rotor. This means that a dynamic eccentricity is a function of space and time. A typical cause of a dynamic eccentricity includes bent shafts, mechanical resonances at critical speeds, and bearing wear. Figure 4 shows an illustration of how the rotor would rotate in the presence of each type of air-gap eccentricity.

Eccentricity faults in PM motors affect certain characteristic frequency components in the machine air-gap magnetic field and consequently vibration and sound power level spectrum radiated from the machine. The dynamic eccentricity causes magnetic flux density component at frequency given by:

$$f_{de} = f_1 + k\frac{f_e}{p} \tag{5}$$

where f_{de} is the dynamic eccentricity frequency, f_1 is the fundamental frequency, p is the pole pair number, and k is any integer.

The proof of Equation (5) is based on the fact that the eccentricities cause change in the permeance. As indicated in Equation (1) the flux density in the air-gap is given by the product of

the field created by magnet (stator winding) and the relative air-gap permeance. Under the initial modeling assumption, the permeance is constant because of the uniform air gap. However, any change in the air-gap length causes a variation of the permeance which can be accounted for by additional harmonics in the permeance function and consequently in the air-gap magnetic field and radial magnetic forces [8].

In the mathematical model the effect of eccentricity is accounted by modifying the expression of the permeance function in the Equation (1), which becoming variable not only in space but also in time:

$$\bar{\lambda}(\theta, t) = \bar{\lambda}_{sl}(\theta)\,\bar{\lambda}_{eccs}(\theta)\,\bar{\lambda}_{eccd}(\theta, t) \tag{6}$$

where $\lambda_{sl}(\theta)$ is the relative permeance that includes the stator slots openings [1], $\bar{\lambda}_{eccs}(\theta)$ and $\bar{\lambda}_{eccd}(\theta, t)$ is respectively the relative permeance that includes the static and dynamic eccentricity and which can be approximated by sinusoidal variation [1, 2].

$$\bar{\lambda}_{eccs}(\theta) = \lambda_{eccs}\cos\theta \tag{7}$$
$$\bar{\lambda}_{eccs}(\theta) = \lambda_{eccd}\cos(w_{ec}t - \theta) \tag{8}$$

And $w_{ec} = w_r$ the angular rotor speed.

By using Fourier series decomposition, and after some mathematical operations we deduce the expression of the parameters λ_{eccs} and λ_{eccd}

$$\lambda_{eccs,d} = 2\frac{1 - \sqrt{1 - \varepsilon_{s,d}^2}}{\varepsilon\sqrt{1 - \varepsilon_{s,d}^2}} \tag{9}$$

$$\varepsilon_{s,d} = \frac{e_{s,d}}{g} \tag{10}$$

e_s and e_d are the static and dynamic eccentricity respectively, g the air-gap length.

Including Equation (6) for air-gap parmeance function instead of $\bar{\lambda}(\theta)$ in Equation (1) we can obtain the magnetic flux density in the air gap of the machine with eccentricity effect taken into account. Figure 5 show the variation of magnetic flux density with and without eccentricity of 4 poles, 36 slots motors.

When comparing Figures 5(a) and 5(b), we note that in the presence of an eccentricity, the magnetic flux density wave is deformed and this is reflected by the presence of other harmonics in the air gap. The interaction between this harmonics according to Equation (2), produce new force waves. The most dangerous are those with a low mode number.
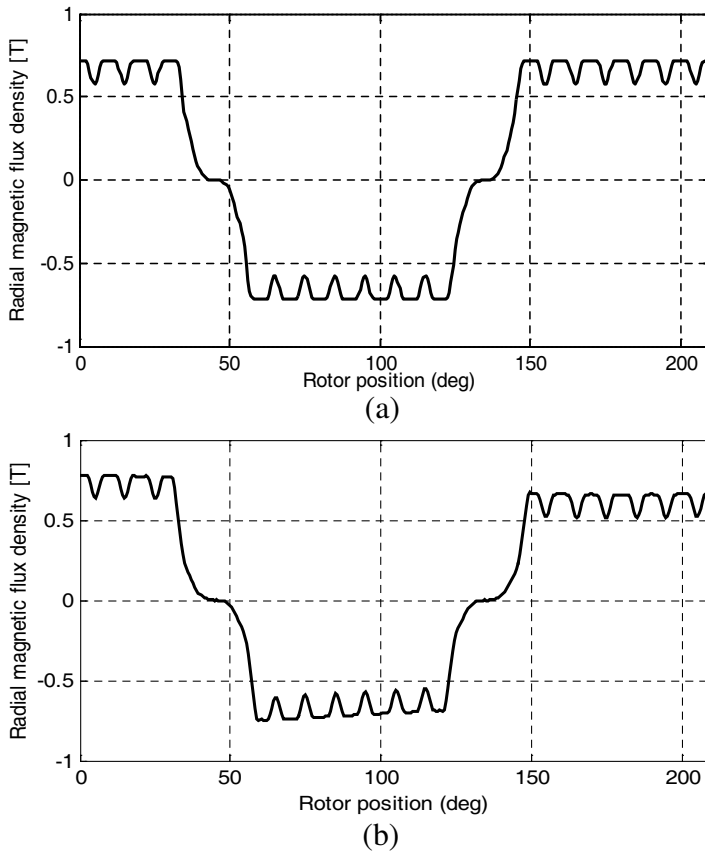
Figure 5. Air-gap magnetic flux density with (a) 0% eccentricity and (b) 25% eccentricity.

4. PREDICTION OF NOISE RADIATED FROM STATOR SYSTEM

The electromagnetic part of model described above allows us to have magnitudes, frequencies, and orders of radial magnetic forces. Noise and vibration of the motor structure are the direct responses of the excitation by these forces. For example if the radial magnetic force is close to one of the natural frequency of the stator system and the order r is the same as the circumferential vibrational mode m of the stator system, significant vibration and acoustic can be produced. The calculation of stator vibration which is considered in this case as 2D ring with free boundary condition is based on the theory of forced vibration with periodic excitation [10].

The vibration displacement of the machine of the mode number and frequency concerned can derived as:

$$Y_d^m = \frac{\pi D_{\&in} L_i P_{mr}}{K_m} \frac{1}{\sqrt{(1 - f_r^2/f_m^2)^2 + 4\zeta_m^2 f_r^2/f_m^2}} \tag{11}$$

The vibration velocity of mode number m is then:

$$V_m = 2\pi f_r Y_d^m \tag{12}$$

where D_{1in} is the stator core inner diameter, L_i is the effective length of the stator core, K_m is lumped stiffness of the stator, f_m is the natural frequency of mode m, f_r is the frequency of the force component of the order r and ζ_m is the modal damping ration. The natural frequency of the stator system can be approximately evaluated as [1]

$$f_{mn} = \frac{1}{2\pi} \sqrt{\frac{K_m^{(c)} + K_{mn}^{(f)} + K_m^{(w)}}{M_c + M_f + M_w}} \tag{13}$$

where $K_m^{(c)}$ is the lumped stiffness of the stator core for the mth circumferential mode, $K_{mn}^{(f)}$ is the lumped stiffness of the frame for
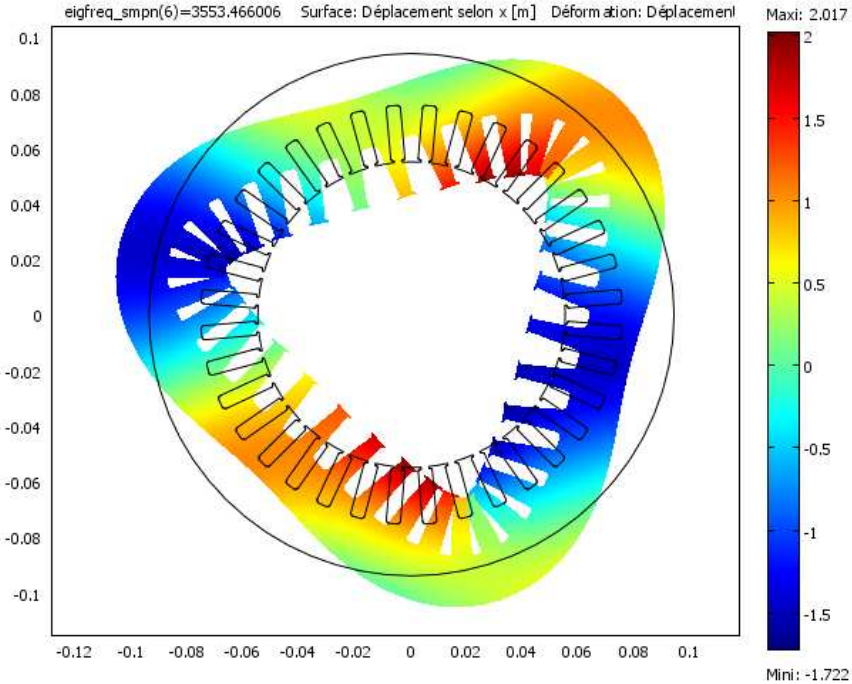

Figure 6. Order 3 mode of PMSM.

mth circumferential and nth axial mode, $K_m^{(w)}$ is lumped stiffness of the stator winding of mth circumferential vibrational mode, M_c is the lumped mass of the stator core, M_f is the lumped mass of the stator core, and M_w is lumped mass stator winding. A numerical validation of analytical calculation of natural frequency was made by COMSOL software. Figures 6 and 7 show how the stator machine is deformed when the vibration modes 3 and 4 are excited.

The vibrating structure of the machine produces sound waves in the ambient medium. Given the outside dimensions of a PM machine, the radiated acoustic power W corresponding to a specific vibration component can be calculated from the relative sound intensity $\sigma_m(f)$, since

$$W_m(f) = \frac{1}{2}\rho_0 c_0 S_c \sigma_m(f) V_m^2 \tag{14}$$

where S_c is the stator outer surface, ρ_0 the air density. Higher vibration levels mean higher radiated sound power. In many cases, however, it is not the absolute value, but $\sigma_m(f)$ which play the role of transfer function from the structural vibration to the acoustic response that
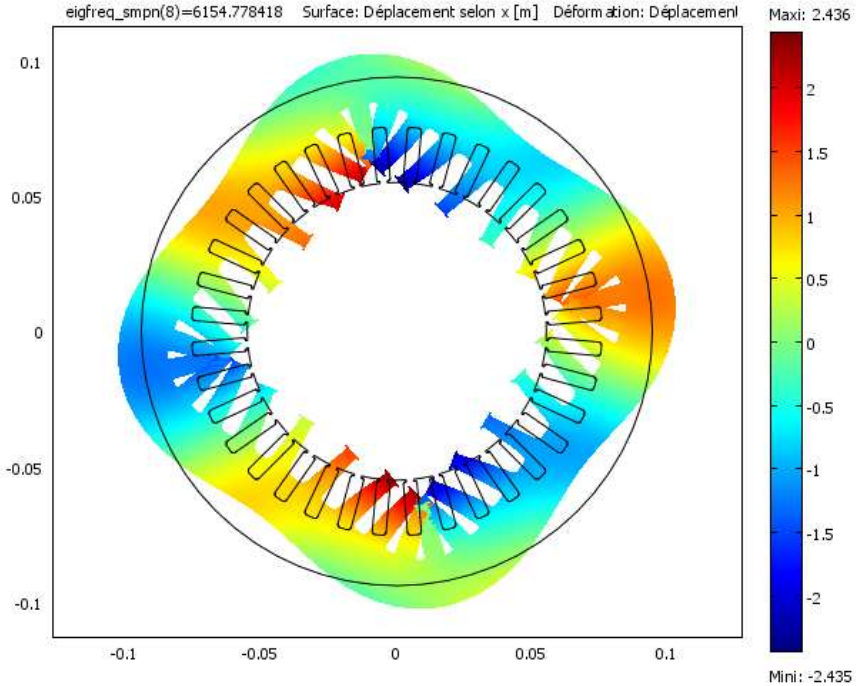

Figure 7. Order 4 mode of PMSM.

is of greatest interest. σ_m is approximated using either its pulsating sphere expression, its finite or infinite cylindrical expression according to stator dimensions [9].

5. SIMULATION RESULTS OF SOUND POWER LEVEL (SPL) WITH ROTOR ECCENTRICITY

Three simulations were made, for 4-poles, 36 slots PM synchronous motors at no load. The inner diameter is $D_{1in} = 165$ mm, stator outer diameter $D_{1out} = 232.5$ mm, effective length of stator 170 mm, air-gap $g = 1$ mm. The rotor magnets are Nd-Fe-B type, magnetized in radial direction. In first simulation where the noise spectrum is shown in Figure 8, the rotor eccentricity was set at 0%, while the motor speed was set at 3500 rpm. In the second the rotor eccentricity was set at 25% and speed to 3500 rpm. In the last simulation the eccentricity was kept at 25% but the rotation speed was increased to 4200 rpm to show the effect of rotating speed.

Note that the natural frequency of the stator system including stator teeth and frame calculated analytically and validated numerically are: 5566 Hz for circumferential mode 0, 991 circumferential mode 2, 2671 circumferential mode 3, 4819 circumferential mode 4. It noted that for a 0% eccentricity (symmetric condition) there are only modes 0,4 and 8, this dominants modes which are predicted by the analytical model results principally from the interaction between PM field and slotted structure of the stator. From Figure 9 and Figure 10 for magnetic noise spectra at 25% eccentricity, we remark that some additional mode of vibration have been introduced, the new mode vibration included modes 3 and 5 resulting from the new harmonics in air magnetic field due to the rotor eccentricity faults. We remark also that rotational speed affects both the frequencies and magnitudes of the sound power level. We remark also that the eccentricity fault may be
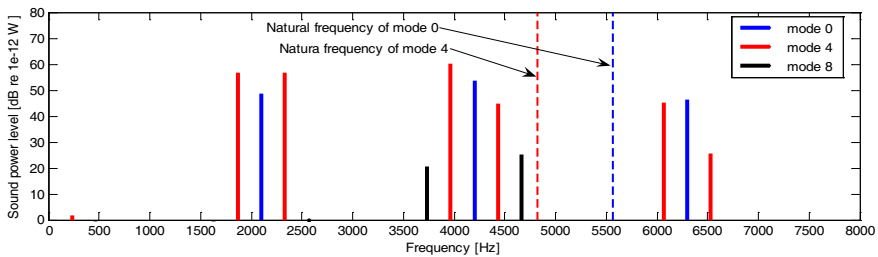

Figure 8. Sound power level spectrum at 3500 rpm and without eccentricity (symmetric condition).
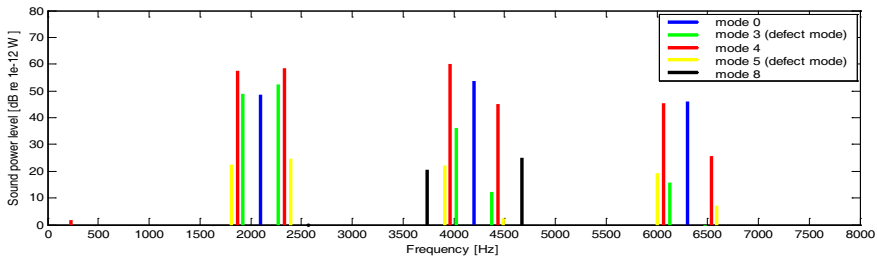
Figure 9. Sound power level spectrum at 3500 rpm and with 25% eccentricity.
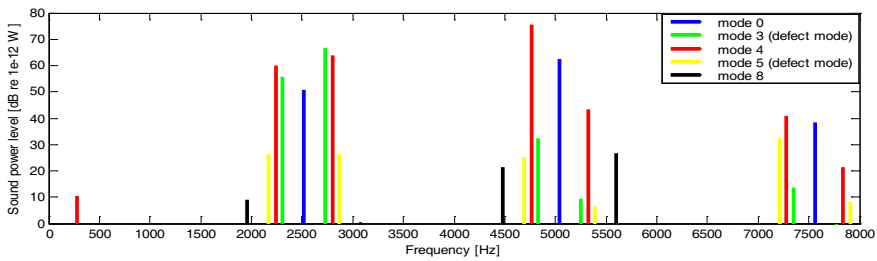

Figure 10. Sound power level spectrum at 4200 rpm and with 25% eccentricity.

very dangerous when the motor is used in variable speed applications, because the frequency of forces waves generated by eccentricity may become close to natural frequency of vibration mode 3 or 5 and the contribution of this mode to the global sound radiated by the machine become very important.

6. EXPERIMENTAL TESTING OF DYNAMIC ECCENTRICITY

This part presents the experimental test bench that has been established with the aim of model validation.

The components of the experimental test bench can be classified into two categories: electromagnetic and electronic.

The electromagnetic components consist of the studied machine (testing) type PMSM, a dc machine and a position sensor type resolver (mounted on PMSM).

The electronic components consist mainly of a three-phase inverter for supplying the PMSM. A system of control in real time (RTI) called DSPACE. This system is built around a DSP running under

the Matlab/Simulink$^®$ and equipped with software called Driving Test ControlDesk, and the acquisition components which running under NI LabView software.

Note that the machine has three pairs of poles placed at the surface of the rotor and separated between them by ferromagnetic material where the B-H curve is presented in the appendix (Figure A1), the rotor of the machine is with magnets inserted. The magnets are Neodymium-Iron-Boron (Nd-Fe-B) type. The other geometrical and physical parameters are presented in Table A1.

To test the dynamic eccentricity, an unbalanced rotor is implemented by mounting a slotted disk on the shaft of the PMSM under test (Figure 11).

A bolt can be positioned at any slot on the disk. So, when the unbalanced disk rotates, the bolt pulls outward as a result of centrifugal force. The rotor is therefore being pulled continuously outward with a force that dedicated by both, the mass of bolt as well as the position of the bolt on the disk.

The vibrations of the outer frame of the PMSM are measured with and without eccentricity using a piezoelectric accelerometer placed on the outer surface of the motor frame. The noise radiated from the machine is measured also with and without disk using a microphone placed at 10 cm from the machine outer surface. The measured data are analyzed using a developed program in software National Instrument NI Lab-View.

Figures 12 and 13 present the sound power level (SPL) of the machine obtained by the developed model and by measurements when the machine is running with a speed of 1500 rpm. As is observed in the Figure 12, in addition to the most dominant predicted noise component; i.e., $6f_1, 12f_1, 18f_1, 24f_1, 30f_1$ ($f_1 = 75$ Hz) which is generated by the radial vibration of the stator, a number of other
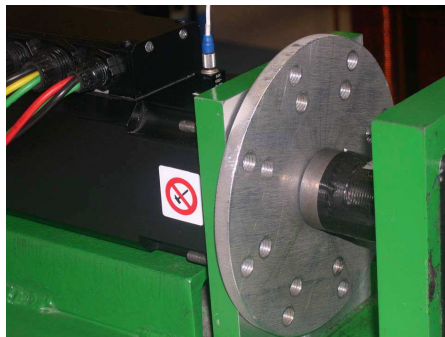

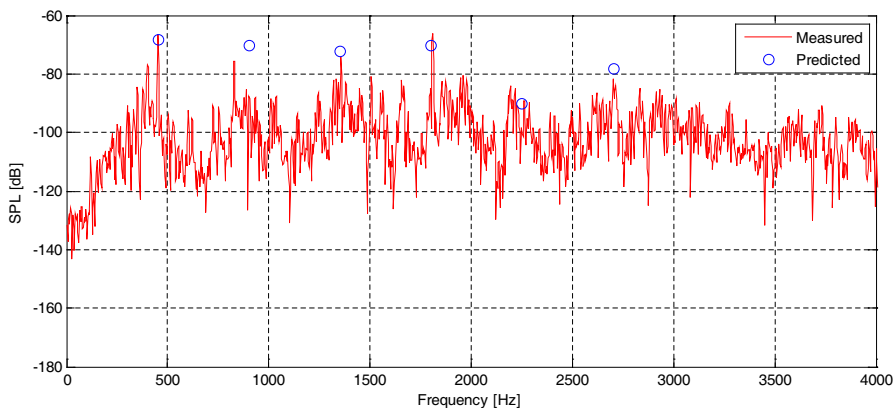**Figure 11.** Experiment test bench of dynamic eccentricity.

Figure 12. Noise spectrum of the machine under test without disk (without eccentricity).
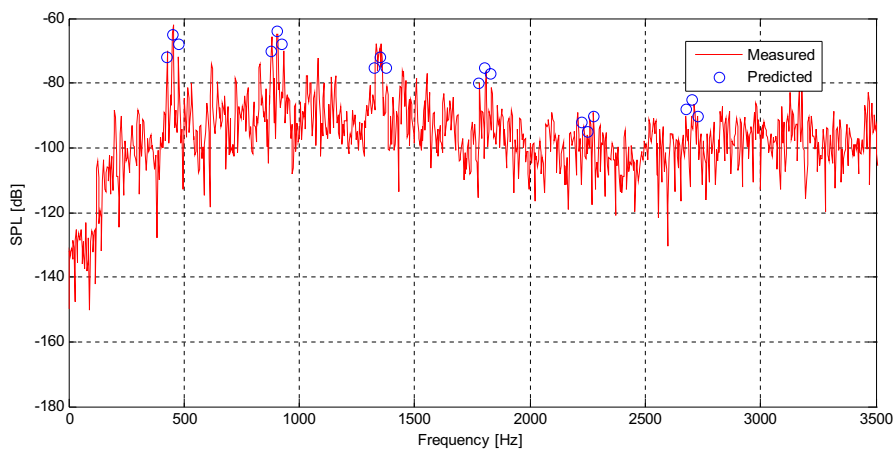

Figure 13. Noise spectrum of the machine under test with disk (with eccentricity).

substantial components have been measured due to authors sources of vibration and natural eccentricity of the machine. The above dominant frequency component predicted by analytical model which is produced purely by interaction between harmonics of air gap magnetic flux density correspond to mode vibration $r = 0$ or "breathing". The model predicts also insignificant frequency do to the fact that this components are of higher mode order, 6, and this is confirmed by measurements.

The measurements confirm in the case of dynamic eccentricity (machine with disk and bolt) the presence of the predicted additional

noise components with frequency $6f_1 \pm \frac{f_1}{p}$, $12f_1 \pm \frac{f_1}{p}$, $18f_1 \pm \frac{f_1}{p}$, $24f_1 \pm \frac{f_1}{p}$, etc. Note that different between measurements and the results of proposed model is due to the imprecision in the estimation of radial forces and the natural frequency of the machine under test, where the geometry of the stator is very complicated.

7. CONCLUSION

In this paper, a noise predictive model of PM brushless motor was presented. The model takes into account the effect of eccentricity via the permeance function as a result the air gap magnetic field contains other harmonics contributes to the generation of low modes of vibration which cause a harmful noise. The experimental works performed on a motor laboratory confirm the apparition of the eccentricity faults signature in the noise spectrum of the investigated machine. The new noise components were identified by the proposed analytical model. The results are encouraging, so we will consider for the remainder of this work the use of the developed model in inverse problem for detecting these defects.

ACKNOWLEDGMENT

APPENDIX A.

Table A1. Parameters of the machine under test.

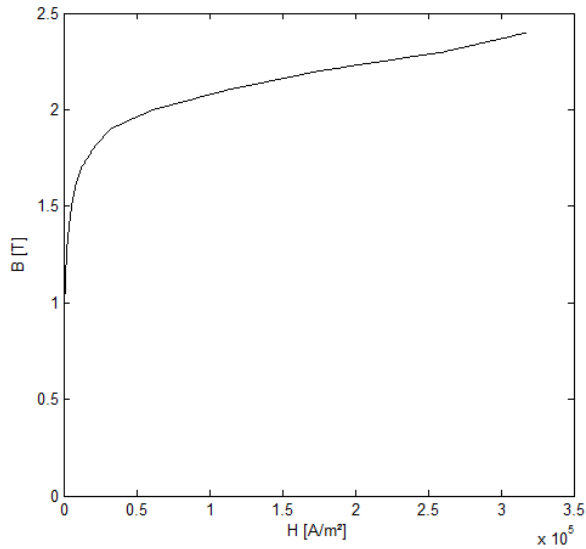| Parameters	values
Number of pôles	6
Stator slots number	18
Stator outer diameter	77.5 mm
Thickness of the stator frame	5.88 mm
Height of teeth	13 mm
Stator lamination Young modulus	$2.06 \times 10^{11}\,\mathrm{N/m^2}$
Slots opening	1.67 mm
Air gap thickness	1 mm
Axial length of the machine	177 mm

Figure A1. *B-H* curve of the ferromagnetic material for the machine under test.

REFERENCES

1. Gereis, G. F., C. Wang, and J. C. Lai, *Noise in Polyphase Electric Motors*, Taylor & Francis, USA, 2006.

2. Zhu, Z. Q. and D. Howe, "Electromagnetic noise radiated by brushless permanent magnet DC drives," *6th IEMDC International Conference on Electrical Machines and Drives*, Oxford, UK, September 1993.

3. Gereis, G. F., C. Wang, J. C. Lai, and N. Ertugrul, "Analytical prediction of noise of magnetic origin produced by permanent magnet brushless motors," *Electrical Machines and Drives Conference IEMDC*, Antalya, Turkish, 2007.

4. Wang, S., M. Aydin, and T. A. Lipo, "Electromagnetic vibration and noise assessment for surface mounted PM machines," *IEEE Power Engineering Society Summer Meeting*, Vancouver, Canada, 2001.

5. Rajagopolan, S., "Detection of rotor and load faults in brushless DC motors operating under stationary and non-stationary conditions," Ph.D. dissertation, School of Electrical and Computer Engineering, Georgia, USA, 2006.

6. Wang, X., Q. Li, S. Wang, and Q. Li, "Analytical calculation of air gap magnetic field distribution and instantaneous characteristics of brushless DC motors," *IEEE Transaction on Energy Conversion*, Vol. 18, 425–432, 2003.

7. Zhu, Z. Q. and D. Howe, "Instantaneous magnetic field distribution in PM brushless DC motors, Part IV: Magnetic field on load," *IEEE Transaction on Magnetics*, Vol. 29, No. 1, January 1993.

8. Maliti, K. C., "Modelling and analysis of magnetic noise in squirrel cage induction motors," Doctoral dissertation, Royal Institute of Technology, Stockholm, 2000.

9. Zhu, Z. Q. and D. Howe, "Improved methods for prediction of electromagnetic noise radiated by electrical machines," *IEE Proc. of the Electric Power Applications*, Vol. 141, 1109–1120, 1994.

10. Norton, M. P. and D. G. Karczub, *Fundamentals of Noise and Vibration Analysis for Engineers*, Cambridge, 2003.